Auxiliary Inflatable Wheels for Lunar Rovers: The AIRWHEEL Project

NASA Big Idea 2024 Final Report

by

Nicolas Umberto Bolatto - Graduate, Aerospace Engineering
Daniil Gribok - Graduate, Aerospace Engineering
Ryan Mahon - Graduate, Aerospace Engineering
Meredith Ashley Embrey - Undergraduate, Architecture
Romeo Gabriel Perlstein - Undergraduate, Aerospace Engineering
Rahul Vishnoi - Graduate, Computer Science
Charles Patrick Hanner - Graduate, Aerospace Engineering
Corbin Yang Voorhees - Undergraduate, Aerospace Engineering
Alan Michael Tchamourliyski - Undergraduate, Aerospace Engineering
Samuel James Heintz - Undergraduate, Aerospace Engineering
Christopher David Kingsley - Graduate, Aerospace Engineering
William Kingsley Covington - Undergraduate, Aerospace Engineering
Lester Cheng - Undergraduate, Aerospace Engineering

Faculty Advisor: Dr. David Akin
Department of Aerospace Engineering

University of Maryland, College Park
Supported by the Maryland Space Grant Consortium

Contents

University of Maryland- AIRWHEEL

Concept Synopsis:

- The AIRWHEEL concept is designed to mitigate the issue of rovers, while traveling, getting stuck in holes, craters, and ditches. The auxiliary inflatable wheel will slow and stop the problem of rigid wheels digging into the soil by not only adding surface area but with the slight give that an inflated structure has to offer. The wheel will, and has shown to, help a stuck wheel remove itself from a ditch, and climb a slope. The wheel also does have the important capability of retraction and reuse.

Image depicting concept

Innovations

- Wireless power and data transfer at the wheel hub removes the need for slip rings in a dusty environment, and allows rapid wheel exchanges
- The use of inflatables on space missions has had issues with maintenance ability and durability. Rigid grousers allow for the possibility of more widespread use of inflatables on missions. This is due to the grousers taking majority of the wear from motion both when in use (unstowed) and during transport time (stowed). Because the inflatable itself does not break down as fast, the maintenance and installation of auxiliary wheel systems can be streamlined.

Verification Testing Results & Conclusions

- When it comes to getting out of a ditch, or climbing a steep slope, an inflated wheel can save a rover from failure, and still get it back home. Our testing has shown that an inflated auxiliary wheel does perform better in climbing slopes and escaping ditches than the rigid wheel alone.
- The use of rigid grousers has also enabled for a more uniform inflation in the system than those without grousers mounted on the wheel. The grousers also enabled for a consistent and tightly packed retraction method, which was not possible without the rigid faces closing the soft goods inside the wheel hub.

I. Executive Summary

Demands on wheeled vehicles in an era of human planetary exploration will greatly exceed those seen to date. Rovers and other surface vehicles will be larger, faster, and more capable, particularly in terms of access to varied terrains and environmental conditions. Experience with Mars rovers represent the most applicable case for future lunar exploration, and demonstrate that terrain conditions are the largest single factor in rover success and longevity. Choosing to drive on sand to avoid the potential damage from rocks doomed Spirit; taking the opposite strategy has shredded the wheels and complicated the operations of Curiosity. As Artemis begins lunar operations planned to encompass permanent lunar bases, truly capable lunar rovers will require adaptability across a wide range of surfaces and temperatures.

Wheels optimized for traversing rocky regions are not well suited to sandy regions, which need lower contact pressures but also benefit from larger grousers for torque transfer. Inflatable "balloon" tires have been repeatedly investigated with good trafficability in sandy terrains, but poor durability and a catastrophic failure mode if a leak occurs. The key premise of the Auxiliary Inflatable Robotic Wheels (AIRWHEEL) project is that it would be good to have inflatable wheels when they are needed in a contingency, but design them to self-stow when the crisis is over so they will be available repeatedly over the life of a rover.

Under the support of the NASA 2024 BIG Idea program, the University of Maryland Space Systems Laboratory has investigated the concept of installing an inflatable wheel extension in the hub of rigid rover wheels, protected from the ambient environment by a segmented outer cover made of spring-loaded wedge elements. If the primary wheel is in terrain exceeding its trafficability limits, the auxiliary wheel can be inflated, both increasing wheel width and contact patch area, while also deploying the rigid wedges with additional grouser patterns to increase soil thrust of the wheel. This concept, originally verified by fundamental terramechanics analyses, was instantiated with a series of prototype wheels of the same approximate size as those on VIPER or Astrolab FLEX. This development process involved multiple prototypes of wheels, grouser petals, and soft goods for inflation, as well as an embedded system for inflation and deflation/stowage based on remote wireless input and using passive springs to deflate the pressure bladder and pull it back into the wheel hub after use.

This concept was tested in three complementary ways: by the creation and use of an instrumented linear wheel test track that provides quantitative measurements of wheel performance in terms of rolling resistance and wheel traction; by the modification of a small rover to accommodate four AIRWHEELs and test them in representative traverses over difficult terrain; and by the installation and testing of a self-contained AIRWHEEL in a thermal vacuum chamber. These tests have been delayed due to challenges in obtaining the second phase of funding under this program, but do show that the AIRWHEEL concept can provide valuable augmentation when the rigid wheel is embedded in sand or trying to climb a slope. Inflatable wheel deployment is highly reliable; retraction has been successfully demonstrated, although further research is needed to refine the use of springs as passive devices to both retract the gas bladder into the wheel hub and help to deflate the pressure bladder during retraction. This was also the case in the vacuum testing. While this document is the culmination of the BIG Ideas competition, the AIRWHEELS team plans to continue to iterate and improve their design, including adapting to larger and more flexible core wheel designs.

II. Problem statement and background

As the Artemis program makes steps towards a permanent human presence on the Moon, the need for mobile lunar systems for logistics, maintenance, and exploration will skyrocket. Under NASA's Moon-to-Mars objectives, lunar infrastructure and exploration goals depend on robust and reliable ground transportation systems for maximizing crew exploration capabilities and economic value. To accomplish this, rovers will be expected to navigate not only the lunar surface features we can measure from space, such as slope geometry and rock scatter, but they must also be effective in a myriad of varying soil conditions that cannot be measured in advance.

In the early 20th century, Karl Terzaghi was one of the first to describe soil mechanics in terms of physical parameters such as cohesion, bearing capacity, and shear strength. Terzaghi [1]—along with the subsequent works of Bekker [2], Wong [3], and Reece [4]—have defined terramechanics formulas that capture the empirical behavior of wheels in varying soils. These foundational works have been largely sufficient for defining vehicle behavior for Earth applications, where vehicle driving errors can be quickly corrected by human operators, but considerable accuracy is necessary for non-terrestrial surface robotics where teleoperation light-time delay exasperates errors, on-board computation is limited, and *a priori* knowledge of soil characteristics is impractical.

Modern rovers can be designed for an intended surface environment with a healthy margin for soil parameter variability, but even so, the entire family of Mars rovers have experienced issues with sudden loose soil ("sand traps") that nearly cause total loss of mobility. Although active traversability-estimating systems are employed on NASA's Mars vehicles to decrease risk [6], rovers are still prone to becoming stuck because predictions are local—they estimate only the rover's current state rather than its future state and do not explicitly estimate slip. As the father of soil mechanics, Karl Terzaghi, puts it: "Natural soil is never uniform. Its properties change from point to point while our knowledge of its properties are limited to those few spots at which the samples have been collected. In soil mechanics the accuracy of computed results never exceeds that of a crude estimate..." [7]. Actually extracting rovers from areas of poor detected stability, weight distribution, or traction is much more difficult. In order to do so reliably, reconfigurability or redundantly actuated systems that can remove rovers from low-cohesion soils may be required [8]. Furthermore, the surface vehicles powering the Artemis program and beyond may require access to areas that demand greater traversability than classic rigid wheels can provide. There have been a number of investigations of inflatable wheels that demonstrate the benefits of inflatables' compliance towards traversing complex terrain morphologies [9] [10], but their advantages are often outweighed

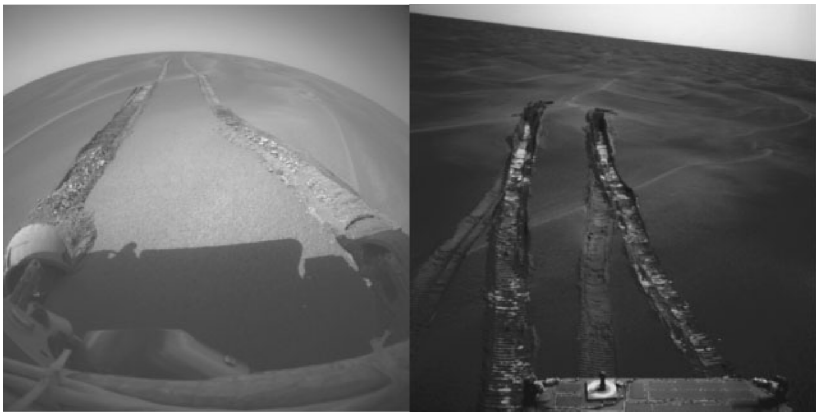

Fig. 1 Images from from Maimone et al. of Opportunity stuck for *five weeks* when encountering particularly loose terrain at Purgatory Ripple [5]. Eventual extrication required retracing its path and avoiding the area altogether.

by their propensity to be easily damaged by rocks and other terrain features.

Thus, the rovers of the future must be capable of adapting to the environment in real-time to combat particularly difficult terrain. Our BIG Idea seeks to address this problem with the creation and evaluation of re-deployable inflatable auxiliary wheels for rovers. These inflatables will, as needed, work alongside classical rigid wheels to increase their effective width, improve weight distribution, and enhance traction thanks to the superior contact patch of flexible wheels. The inflatable portion will be deployed for exclusive use in areas of poor trafficability, where the rover would otherwise experience deep sinkage, high wheel slip, or possibly even complete immobilization. Once the rover is back in conventionally navigable terrain, the inflatable wheels are no longer needed and will retract to prevent unnecessary wear and tear on the comparatively delicate inflatable membrane. This concept is further augmented by the inflation mechanism also deploying intermittent rigid rim elements, which allow the use of extended grousers for increasing torque transfer to the soil beyond that feasible for classic inflatable planetary wheels.

In classical terramechanics theory, soils are modeled as nonlinear springs, and quantified by coefficients of cohesion and internal friction as well as the exponent of the nonlinear spring deflection. Under this approach, there are four major factors contributing to rolling resistance. Gravitational resistance is related to the slope angle, and internal friction resistance to the wheel mechanisms. Of greatest interest in this problem are the compaction resistance and bulldozing. Compaction resistance relates to work performed by compressing the soil that is rolled over, and is reduced by wider wheels with lower pressure on the wheel-soil contact patch. Bulldozing is the tendency of a wheel to push soil ahead of itself, increasing the overall resistance as the wheel is continually driving "uphill", which is reduced by narrower wheels. The scale of these effects is greatly driven by the soil characteristics, as well as the weight supported by each wheel.

A separate issue is the ability of the wheel to transmit the torque of the drive motor into shear force in the soil, producing thrust for accelerating and sustaining the rover velocity. Smooth wheels are best for rigid surfaces, but looser surfaces provide more traction when the wheels have grousers, or cleats, that cut into the soil and increase the bearing load to sustain ground thrust. The overall figure of merit is "drawbar pull", a term that derives from the use of terramechanics to design farm equipment, but it is just the positive margin of traction thrust over rolling resistance. Drawbar pull must be non-negative to sustain motion, and positive to allow acceleration.

A combination of our own theoretical terramechanics studies and existing work on flexible wheels support the AIRWHEEL concept for improving performance in loose soil. Working in the static regime with theoretical terramechanics models, wider wheels appear to always ameliorate soil-compression resistance when compared to thinner wheels of the same diameter, as shown in Figure 2. This makes sense as wider wheels are better at distributing rover weight across the soil contact patch, and the analysis shows they result in rover wheels sinking less into the ground. This feature of wider wheels is particularly favorable in terrains with low cohesiveness where rovers are prone to excessive sinkage and loss of traction. Furthermore, work by Wong and Apostolopoulos shows that flexible wheels, like those deployed with our project, are substantially more capable of producing traction due to deformation increasing soil contact patch area [3, 11]. Our inflatable designs will aim to take advantage of this property by adjusting tire pressure with respect to weight on the wheel to achieve a balance between sufficient contact patch and minimal rolling resistance.

III. Project Description

A. Concept Development

The initial concept for this study could be summarized as "inflatable wheel augmentations". The multi-year duration for most rovers mitigated against an all-inflatable wheel, as any appreciable amount of leakage would require more inflation gas than would be feasible to transport for lunar exploration, and an ongoing refill operation for Mars even if the atmosphere itself was used as the source of inflation gas. The concept developed as an inflatable system mounted in the wheel interior and inflated upon need: for example, when the wheel threatens to get stuck in difficult terrain. Once the rover has extricated itself from the problematic region, the inflatable wheel augmentation would retract back into the wheel hub in preparation for the next time it is needed. (It was always recognized that the retraction and repackaging requirement would be the most difficult design problem of the project.)

The first trade study was to decide on the baseline wheel prior to augmentation by inflation. It was decided to use a rigid wheel, which is more common to uncrewed planetary exploration rovers than human rover systems, but which offers the advantage of greater interior volume to stow the inflating soft goods, pressurized gas tanks, and associated systems. The rigid wheel is also more amenable to terramechanics analysis, and is more easily modified by changing the number, height, and shape of grousers to increase shear forces into the surface to increase wheel thrust and, ultimately, drawbar pull. This led to the associated decision on the prototype wheel size. Larger wheels would be easier to integrate the inflation system inside the hub, but the plan for rapid redesign and fabrication of test wheels argued for a size capable of additive manufacturing in existing fused deposition printers in the UMd Space Systems Laboratory. The final decision was to focus on 30 cm diameter wheels, as used on TRAVELS, the wheel-on-limb system developed by UMd for the 2022 BIG Idea competition. This started us off with a large supply of test wheels, as well as being capable of printing in a single piece on several large-scale printers in the lab.

The next major decision was the specific implementation of the inflatable auxiliary wheel. Initial designs were completed for an entirely inflatable wheel outboard of the standard rigid wheel, which has the advantage of a larger contact patch with the surface and the capability to have a different inflated diameter from the rigid wheel. It was discovered, however, that the open wheel hub did not provide any protection from regolith infiltrating the stowed wheel fabric, and the lack of external structure made autonomous stowing problematic. Flexible wheels typically reach full tractive force from surface deformation, and this was also limited in proximity to the rigid wheel hub.

The final design included a set of wedge-shaped rigid tread segments hinged on the periphery of the rigid wheel, which are pushed outwards by the inflation of the auxiliary wheel and which provide a spring-loaded force distributed around the wheel hub, which in turn stows the deflated soft goods back into the wheel hub for future reuse. These wedge elements form a hard outer shell over the inflated wheel unit for protection wen stowed, and can be designed with auxiliary grousers to increase tractive force when deployed. While all of the design options considered were tested, the inflatable wheels with hinged rigid wedge segments evolved into the prototype design.

B. Terramechanics Analysis

Terramechanics is the underlying theory of wheel-soil interaction, and forms the basis of the theoretical analysis used in this project. A full derivation of terramechanics theory would more than

fill the entire allotted page count for this report; we present here the essential top-level summary of the analytical approach, based in general form on the seminal work by Bekker[2] with numerous additions from other thought leaders in the field including Wong, Muro, and Iagnemma.

Regolith can be modeled as a nonlinear spring of the form $P = kz^n$, where P is the pressure exerted by the soil, z is the depth of sinkage, and n is an exponent relating to the change in resistance with depth. The "spring constant" k is more typically separated into elements based on soil cohesion k_c and internal resistance k_ϕ, resulting in the form of the soil pressure generally used,

$$P = \left(\frac{k_c}{b} + k_\phi\right) z^n \tag{1}$$

where b is the width of the wheel.

Resistance to the wheel rolling over the surface can be attributed to four factors. Rolling resistance R_r is a function of the internal friction of the rover mechanisms and can be ignored for our purposes here. Gravitational resistance R_g is directly caused by the component of the gravitation vector parallel to a slope, which is not intrinsic to the wheel itself. The two elements of resistance specific to the wheel are compression resistance R_c and bulldozing resistance R_b, which is due to soil pushed ahead of the wheel analogous to the wake of a boat in water. These can be calculated as

$$R_c = \frac{1}{n+1}\left(k_c + bk_\phi\right)^{\frac{-1}{2n+1}} \left(\frac{3W_w}{(3-n)\sqrt{d}}\right)^{\frac{2(n+1)}{2n+1}} \tag{2}$$

$$R_b = \frac{b\sin(\alpha+\phi)}{2\sin\alpha\cos\phi}\left(2zcK_c + \gamma z^2 K_\gamma\right) + \frac{\ell_o^3\gamma}{3}\left(\frac{\pi}{2} - \phi\right) + c\ell_o^2\left[1 + \tan\left(\frac{\pi}{4} + \frac{\phi}{2}\right)\right] \tag{3}$$

The other issue of importance is the ability of a wheel to transfer its torque into soil thrust, which involves creating a shear field under the wheel. The tractive force H in its generic form can be calculated by

$$H = \left[b\ell c\left(1 + \frac{2h}{b}\right)N_g + W\tan\phi\left(1 + 0.64\frac{h}{b}\arctan\frac{b}{h}\right)\right]\left[1 - \frac{K}{s\ell}\left(1 - e^{-\frac{se}{K}}\right)\right] \tag{4}$$

This equation includes the effect of grousers, which are radial plates which project normal to the surface of the wheel and increase the shear volume under the wheel, thereby increasing soil thrust. The key elements of grouser design are represented in this equation: the number of grousers in contact with the soil N_g and the height of each grouser above the wheel circumference h.

These equations, along with the associated ancillary equations used to calculate the various input parameters, form the core of the theoretical terramechanics analysis used for the initial design efforts. While the focus of this paper is on the results of the experimental efforts, a sample of the output of basic terramechanics trade studies is shown in Figure 2.

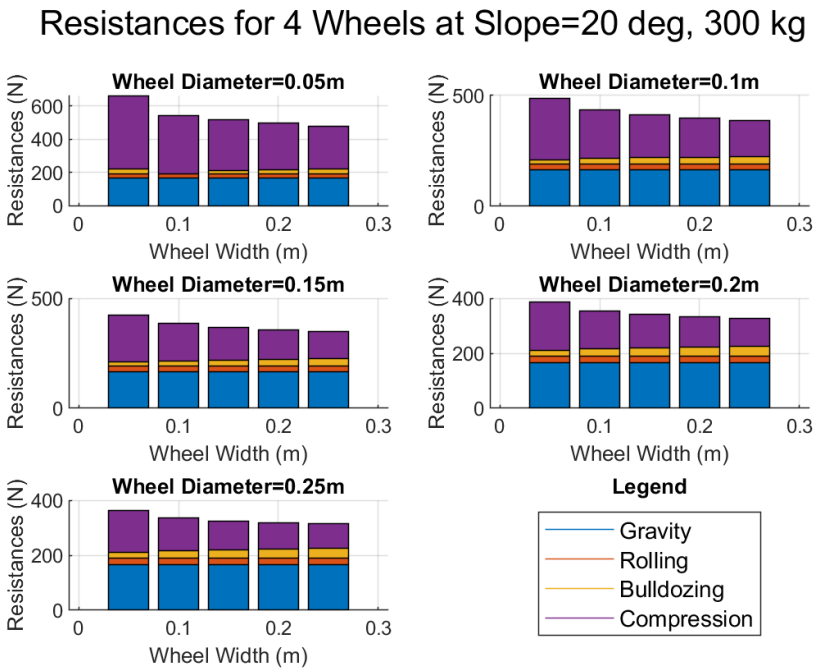

Fig. 2 Terramechanics soil resistances for a variety of wheel geometries, with wider wheels experiencing less overall.

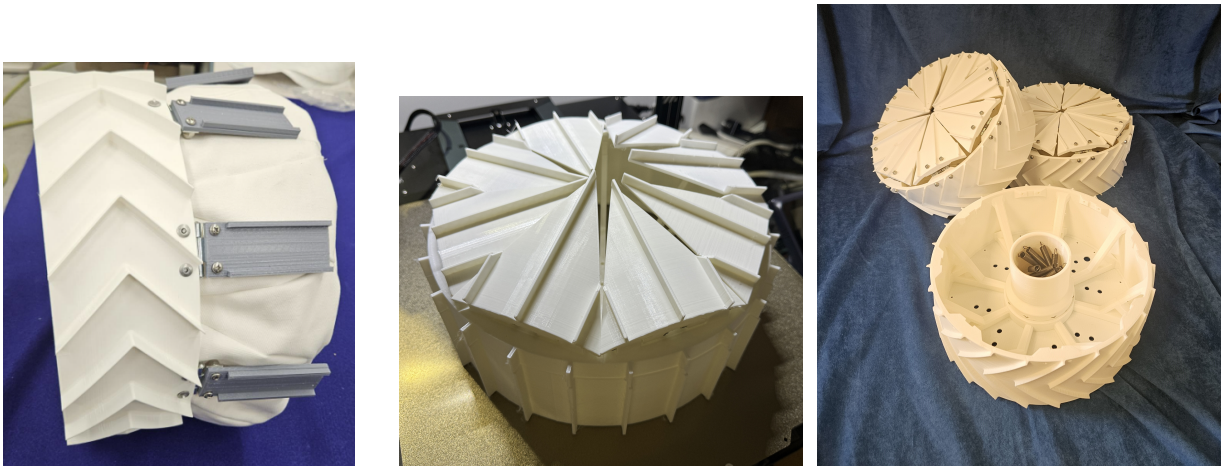

Fig. 3 Design development for full-scale wheel testing – (left) prototype of rectangular tread/grouser extensions in extended configuration (center) triangular grousers in stowed configuration (right) final design for wheel structure with off-center spokes and central axle for inflatable and instrumentation storage

C. Prototype Wheel Design and Fabrication

The use-case for this inflatable rover wheel system is on an unmanned rover operating in sloped, loose soil. Designed for this environment, a VIPER class wheel (30 cm diameter, 4 cm width) inspired the rigid structure of this design and a test case to compare with our inflatable system. This

structure was 3D printed on an FLSUN V400 with a 30cm diameter print bed. The speed of the V400 reduced the print time of a single wheel from 2 days to 18 hours when compared to a Creality printer. Utilising this printer increases the prototyping speed while limiting the rim-to-rim diameter of the wheel to 28 cm with 1 cm tall chevron grousers. 5 Inside of the structure, off-centered wheel spokes increased the internal storage volume from 3.5 liters to 5.06 liters.

On the rear face of the wheel are mounting patterns for the internal subsystems. The inflatable restraining layer is mounted just inside the wheel rim. Bolt holes for securing the CO_2 canisters are placed between spokes for safe mounting of a pressure vessel. The center most bolt patterns allow for mounting the wheels on two different traction motors, the RMD-X8 Pro on our linear wheel test rig and the Robocity motors on our four wheel rover test bed. A bolt pattern for a removable central cylinder which keeps the inflatable oriented correctly during inflation by providing a center axle and prevents interaction between the retraction springs and inflatable fabric during retraction. 4 These grouser retraction springs are mounted to the wheel structure inside of this cylinder preventing pinching and allowing for safe wheel assembly as there is no tension in these springs until the center cylinder is mounted which is done entirely external after the wheel is assembled through heat set inserts on the back of the structure. These modifications to a classic rigid rover wheel create a modular support structure for inflatable testing to become an entirely self-contained hybrid rover wheel armed with an adaptive, lightweight inflation system. 12

D. Retraction Mechanism and Petal Design

The lack of atmospheric pressure makes deflation and re-stowing of the inflatable soft goods challenging. To overcome this lack of pressure differential, we designed a passive spring mechanism which pulls eight grousers evenly back into the wheel. Each grouser is attached to two springs. One torsion spring is integrated into the hinge at the base of the grouser where it connects to the rim of the wheel. 6 The second spring is a tension spring which connects the tip of a deploy-able grouser petal to the central cylinder inside of the wheel. The inflation of the pressure bladder overcomes the spring force as the inflatable wheel deploys. During deflation, a gas solenoid opens the pressure bladder to the surround environment and the spring's restoring force pulls the petal at these tow points which compresses the bladder and pushes it back into the wheel structure.

The deploy-able petal designed for this retraction mechanism use triangle petals the length of the of the wheel radius to protect the soft goods inside of the wheel during the inflatable system's stowed state. In the deployed state, the grouser petals protect the inflatable from rocks and harmful terrain. The grousers on these deploy-able petals were decided to be straight grouser as the results in the highest tractive force at high slips which will be beneficial in this systems use case to increase overall wheel traction. In the deployed state this deployed grouser petal takes inspiration from Curiosity who utilised a combination of straight and chevron grousers in their wheel design. 10

E. Soft Goods Design and Fabrication

The soft goods packed inside of the base rigid wheel are able to be mounted to the back panel of the wheel around the inner circumference of the wheel using 4/40 bolts and 4/40 nylon locking nuts. The pressure bladder, made of polyurethane coated nylon fabric, is heat sealed by hand. The restraint layer, made of 500D cordura fabric, is sewn using a machine. While both 500D and 1000D cordura fab were used in testing, the final wheels with grousers attached use the 500D fabric because of its thin footprint and high tear resistance. The pressure bladder is secured to the restraint layer

Fig. 4 Restraining Cylinder before wheel integration

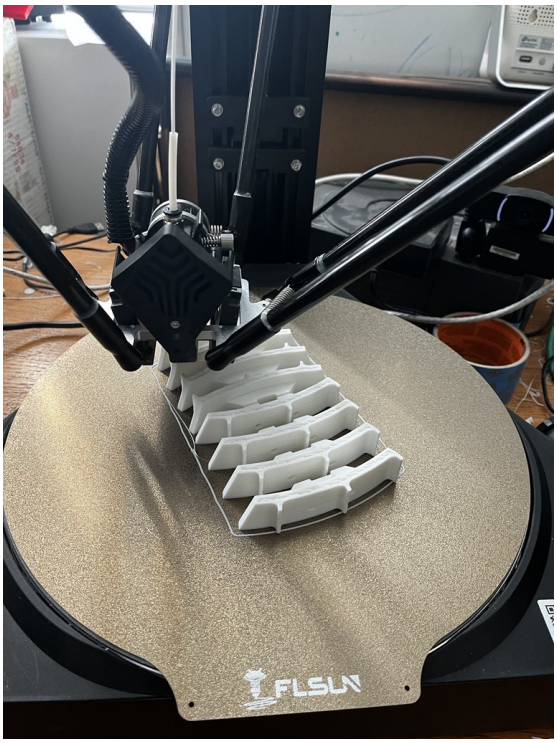

Fig. 5 Rigid grousers during the printing process

along the inner front face seam, using 1/4 inch grommets for added security. This is to mitigate twisting of the bladder within the restraint layer during retraction and inflation.

Three different pressure bladder designs were created and tested alongside two restraint layer designs before landing on the final versions. The restraint layer maintained its triangle reinforced front face, but the final wheels only have a single piece for the outer face of the wheel. The final restraint layer also contains a center hole for easy of mounting to the test rig. There is no internal restraint layer as we have a rigid cylinder in the center of the wheel instead. This design can be seen in Figure 10.

The pressure bladder has more variety in shape. The first iteration, a fully toroidal bladder, was proven difficult to properly seal and to integrate with the wheel for testing on our test rig. The final shape is a tube which is curled around the center axis, and is secured on either end to itself to remain in a circular shape. The shape was decided due to the ability to thread the deflated bladder inside of an already assembled grouser wheel, and for the consistency in construction of the bladder itself. This bladder, for our purposes, has 2 final sizes. The CO_2 testing size, less wide, and the test rig size, larger. The smaller bladder was made to give space to the electronics and inflation mechanism for the self inflatable wheel. Both can be seen in Figure 9. These two final varieties were found through both measurement and trial and error in the integration process.

F. Inflation System Design and Fabrication

The inflation systems for the wheel were designed in stages, and set up to meet testing requirements before meeting flight design requirements. The first system was simply an industrial air regulator

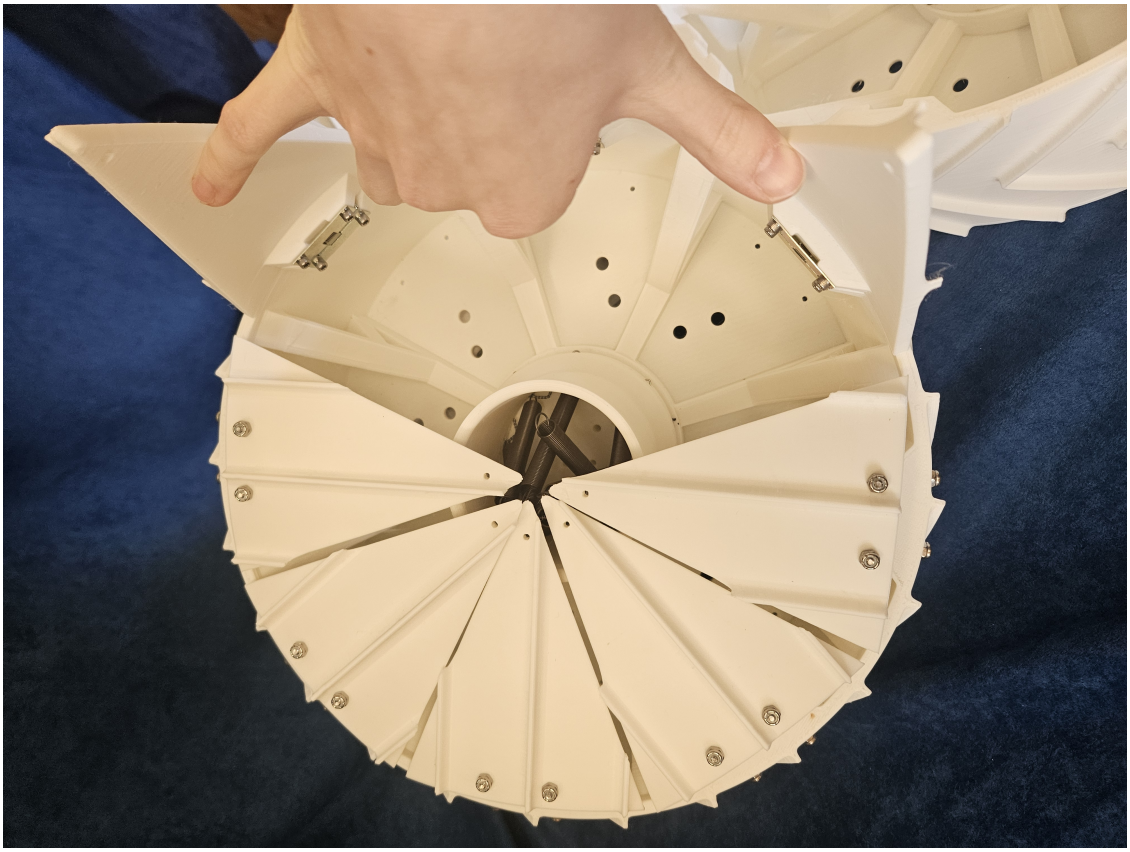

Fig. 6 Holding opening up spring loaded rigid grousers to show restraining cylinder and springs inside

hooked into an air solenoid control valve that provided inflate/deflate paths for the air, and pressure control. This system was not reflective of a flight platform, but was instead designed to make testing inflatable designs easy and safe. The lab has connections to pressurized (120 psi) air, which is in relatively unlimited supply, and safer than CO_2 due to being delivered at a lower pressure. Carbon Dioxide was chosen as the inflation gas for self-contained inflating wheels. The advantages of CO_2 are that it stores in liquid state at room temperature and pressures above 800 psi, resulting in a very high expanded-to-stored gas volume ratio. Alternatives such as compressed air at 3000 psi, commonly used for SCUBA equipment, did not have the same storage density and incurred mass and volume penalties due to the higher pressures. Other liquefying gases such as propane were not used to to their flammability. Figure 11 shows the general layout of the self-contained inflation system, and figure 12 shows the system installed in a wheel. A standard, COTS 25 gram CO_2 cartridge was used for the testing, which allows for 2 inflations of a wheel. The pressure from the cartridge is reduced by a regulator, before being piped to two gas solenoids. The two solenoids are controlled by two receivers, allowing for inflation, deflation, pressure hold, and vent. The pressure hold feature allows the system to shut off both solenoids to conserve power while inflated or deflated. The vent feature is used to vent any remaining gas from the CO_2 cartridge, to allow for partially depleted cartridge to be removed. This system uses two COTS wirelesss tx modules for wireless control with the full understating that a flight system may encounter difficulties integrating a mission-critical wireless communication system. However, the COTS system implemented here serves the purposes

Fig. 7 A variety of the restraint layers produced and tested

Fig. 8 Testing the performance of a deployed inflatable without grousers

Fig. 9 The final two pressure bladder designs

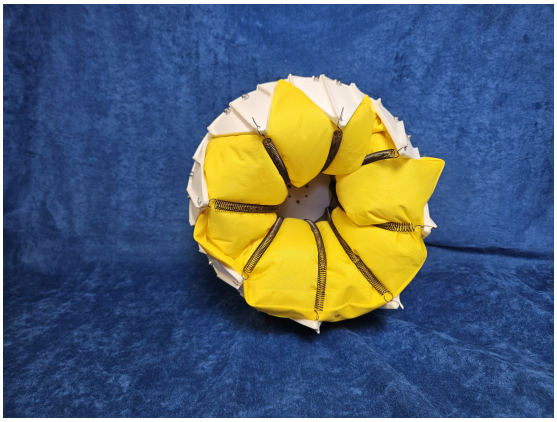

Fig. 10 Inflated wheel with grousers attached

of demonstrating the CONOPS of our Big Idea.

One of the considerations when using a liquefied gas as an inflation media is the cooling effect that occurs when it is discharged and boiled from its container. The location where the material transitions from liquid to gas incurs the greatest amount of cooling due to the aforementioned forced boiling and evaporation. For CO_2 systems, this typically happens at an orifice plate located in a convenient spot where the cryogenic liquid CO_2 won't cause damage, and where a large thermal mass or heat source is available. Unfortunately, due the design of the pressure bladder, the schrader valves used could not have an orifice plate affixed, so the gas expansion had to happen elsewhere. This, alongside the lack of small form equipment to handle liquid CO_2 led to the decision to have the CO_2 boil off in the canister, and have the remaining mass of the CO_2 and regulator assembly provide the heat. While this is not an ideal outcome, it allowed the system to easily fit within the confines of the wheel, and avoid the heavy metal plumbing needed to move 800 PSI CO_2. If the regulator was to experience unacceptable levels of freezing, a small heating element could be installed to heat

it. This type of solution is common in industrial applications, and could be easily supplied by the onboard batteries due to the low duty cycle of the inflation system.

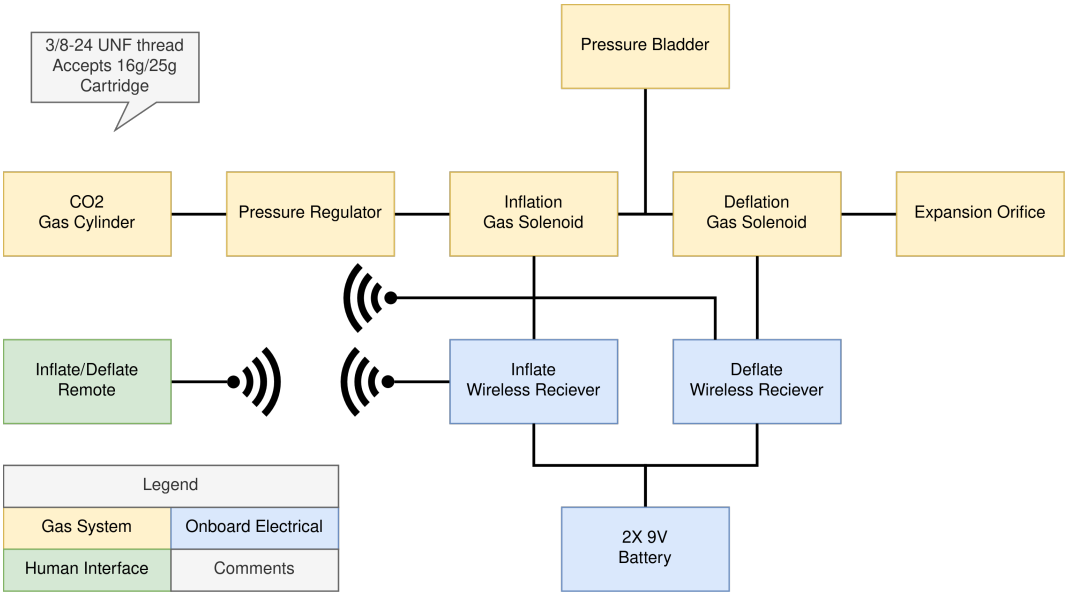

Fig. 11 System block diagram of wheel inflation system

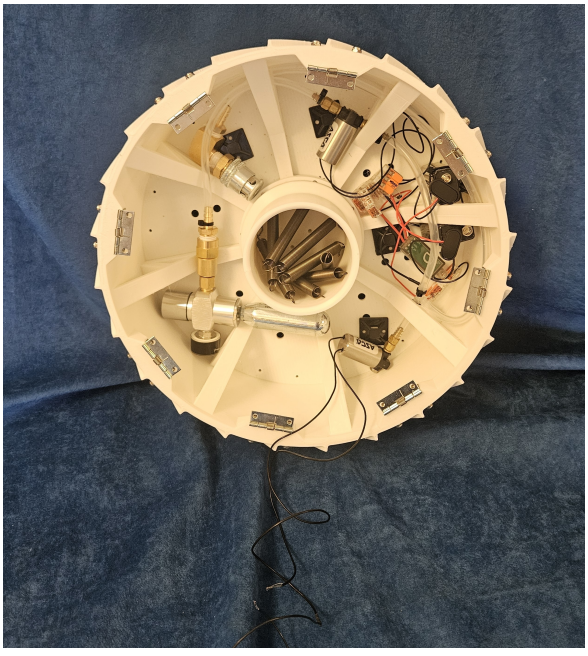

Fig. 12 Internal wheel plumbing for remote CO_2 inflation

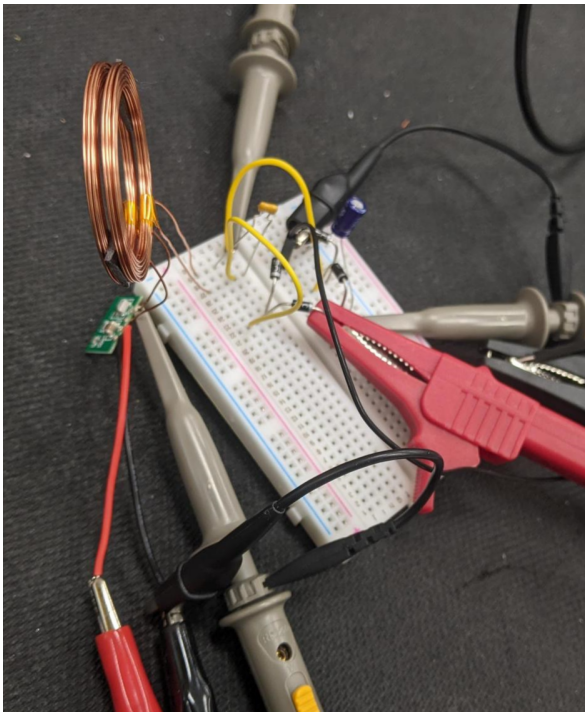

Fig. 13 Coupled induction coil test setup demonstrating gas solenoid actuation via near-field wireless power transfer

G. Wireless power transfer to wheel

One of the prevailing problems with enclosing inflation equipment inside the wheel is that power must be provided to the equipment inside the wheel to actuate valves and provide feedback on system status. Two possible options exist: either passing power and data to the wheel via slip ring, or housing power sources onboard the wheel and communicating via wireless means. While a full trade study between the two options was not conducted, we did observe some qualitative differences between the two implementations. The slip ring system is electrically simpler, but is susceptible to fouling via lunar regolith. A wireless system is electrically more complex, but can be hermetically sealed against dust intrusion. A major downside to the non-slip ring in-wheel system is that power and data must be provided to the electronics inside the wheel with functionally no connection to the rest of the rover. These electronics must survive high vibration and thermal cycle loads, as they would be located outside of the rover chassis. This environment precludes the use of batteries or other storage devices in the wheel. A battery big enough to power heaters to keep itself warm would quickly consume all viable space in the wheel, and eat into the total vehicle mass budget. Technologies such as solar panels are infeasible for our wheel design due to dust collection (wheels are perhaps the worst place to mount solar panels due to the dust they kick up), as well as our concept of operations. Solar panels favorably mounted on the side of the wheel would wind up as driving surfaces once the wheel inflatable is deployed. For these reasons, we investigated a wireless power delivery system, where power is provided on-demand to the electrical system inside the wheel using a pair of inductively coupled coils. A single stationary coil is mounted on the chassis side of the vehicle, concentric with the axis of rotation of the wheel. A second coil is mounted inside the wheel, as close as possible to the stationary coil. When the wheel has to be inflated or deflated, the vehicle coil is energized at a particular frequency, and the wheel mounted coil begins to electrically resonate. The resulting AC waveform on the output of the wheel coil is rectified by a full bridge rectifier, and sent to an electric solenoid that permits either inflation or deflation. A prototype of the system is presented in figure 13. It shows a COTS (Commercial Off The Shelf) wireless power transmitter hooked into a custom tuned resonant circuit. The system successfully transmitted power at a 40% efficiency across a distance of 2mm. While the input frequency was not changed in the setup, it can be modified to accommodate the resonant frequencies of whatever could size is used.

IV. Verification Testing on Earth

A. Verification Process

The verification testing for the AIRWHEEL concept consisted of three major objectives:

- Quantify the performance of the wheel to allow iterative advancements in the concept
- Assess the performance of AIRWHEELs on a rover in representative terrain
- Verify that the system will work in space

To this end, the AIRWHEEL team designed and fabricated a wheel test system that can directly control slip while measuring forces on the wheel. This system was used to test wheel prototypes, and different approaches to the inflatable portions of the wheels. An existing small rover (rocker suspension with four-wheel steering) was modified to accept the 30 cm diameter wheel size decided upon for prototype testing, and used to investigate the utility of the AIRWHEEL concept in loose sandy soil. Finally, a self-contained AIRWHEEL system including CO_2 inflation/deflation system and wireless radio control was testing in the lab's thermal vacuum chamber. Each of these are presented in more detail below. Video clips of these tests are in our tech demonstration video `https://youtu.be/doYxkWzVJNM?si=yCCkL5Hv3N-rILyM`

B. Wheel Test Rig

The key to being able to rapidly and repeatably compare the performance between various wheel designs lies in the creation of our single-wheel linear test rig. Because our project concept requires the wheel to work well for rover propulsion in both the retracted and deployed states, a significant portion of the project has relied on perfecting this testbed.

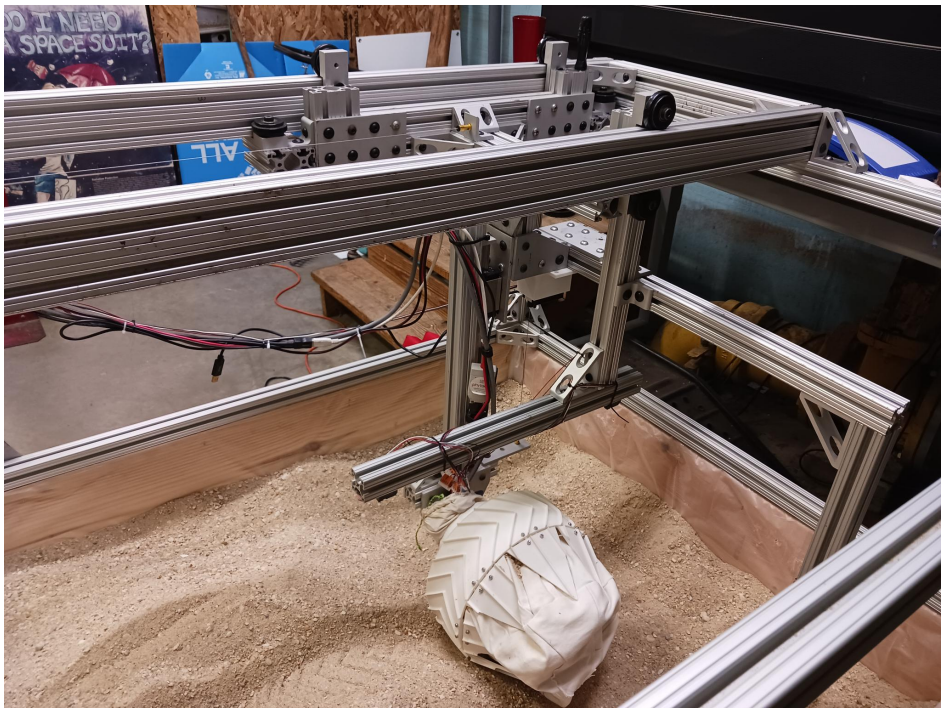

Fig. 14 Overall view of the wheel carriage system in a free-slip test

1. Mechanical Design

The testbed consists of a 2×1 meter sandbox with an overhead 8020-extrusion frame. A a drive motor propels any given wheel down the length of the sandbox, while a sensor mounted to the motor collects 6-axes of force and torque experienced by the wheel during its travel. Rather than remaining at a stationary height, the wheel assembly is mounted to a vertical linear rail to allow the wheel maintain accurate ground contact as it rolls over any terrain features or bumps. This single-wheel assembly is supported by a carriage and set of horizontal rails above, which can either be kept as a passive motion axis to allow the collection of true slip values for given wheel and soil parameters, or the horizontal axis can be actuated to dictate a wheel slip ratio.

While a test rig with actuation only in the wheel is useful for many of our preliminary testing goals, additional actuation for the horizontally-moving carriage would allow the wheel slip variable to become selectable in our tests. This is especially useful because wheel slip is generally an unknown parameter in the field, as it can vary widely based on specific soil properties or vehicle orientation and loading conditions. An actuated carriage therefore allows the evaluation of our inflatable system across any slip value that may be created by differential motion between the wheel drive motor and horizontal carriage. To accommodate for the long travel distance of the wheel test rig's carriage, a rack and pinion system was created and integrated using combinations of COTS components and custom bracketing to minimize design overhead and maximize reliability. The carriage utilizes 2 meters of a steel rack mounted to an 8020 frame beam, with a pulley and pinion system driven by a brushless stepper motor.

Both the passive vertical motion axis of the wheel and the horizontal carriage are equipped with linear encoders to perfectly track the true motion of the wheel across the testbed. A pair of infrared distance sensors ahead and behind the wheel were also mounted to measure soil compression as the wheel travels (Fig. 14). A combination of fabric and 3D printed covers were created to protect the force/torque sensor and wheel motor from sand and dust ingress experienced in the initial tests (Fig. 15).

2. Electrical

The electrical system, while down-scoped from the original plans outlined in the proposal, still received major upgrades. These changes included an overhaul of the control and data acquisition system, installation of a powered horizontal traverse system, and upgrades to the power supply system. These changes were designed to compensate for several deficiencies and fulfill desired capabilities unidentified in the early revisions of the test rig. Of the changes, the addition of the powered horizontal traverses was the most important one, serving as the high level requirement that resulted in the majority of the electrical upgrades. To support the addition of a 800W brushless servomotor for the horizontal traverse, a new motion control card was installed into the system. The Galil DMC-4143 card is an 4 axis servo control card that allows for 4 servos alongside so digital an analog I/o to be controlled with Ethernet. The card was used as both a motion control platform for the horizontal, as well as a data acquisition system for the IR soil distance sensors. Due to the increased power requirements, the power supply system received an overhaul. A 36V, 14A power supply was installed alongside an E-stop system to provide power to both the traction and horizontal motor, while a dedicated 24V power supply powered the Galil motion control card and other small data acquisition electronics.

Fig. 15 The force/torque sensor now has an environmental protection garment, and the wheel drive motor has a 3D-printed cup to protect from sand and dust

3. Software

The first single-wheel tests shown in our last report consisted of manually entering a “start" command and a “stop" command when the wheel roughly reached end of travel on the test rig (often resulting in collisions with hard stops). Since then, software has been created to drive the wheel motor intelligently based on user-inputted parameters and received hardware telemetry, while logging the data from the array of sensors on the test rig. We used the Robot Operating System (ROS 2)’s Data Distribution Service as the middle-ware for data collection and management. Currently, the array of data being collected is as follows: time, commanded motor speed, true motor speed, motor current, motor encoder position, 3-DOF force measurements, 3-DOF torque measurements, wheel horizontal position/velocity in rig, wheel absolute vertical position/velocity in rig, distance to soil in front and behind the wheel. At the end of a run, data is written to a CSV for future processing. The results of this data are shown in section IV.C.

C. Wheel Performance Testing

The single-wheel test rig allowed exhaustive testing of our different wheel designs. By additionally manipulating variables such as weight-on-the-wheel, slip, speed, terrain geometry, and inclination, we were able to evaluate performance in a variety of situations. Throughout an experiment, the test rig collects data on: time, wheel drive encoder position, true wheel position and velocity horizontally and vertically (used to calculate slip), 6-axis force and torque measurements at the wheel, and infrared distance sensor readings on the soil in front and behind the wheel.

One important component of performance testing was matching the weight-on-the-wheel of the class of rovers that match our project’s intended use. Since traction and resistance is proportional to the force of the wheel on the soil, we manipulated this variable throughout testing by directly adding

and removing lead weight from the test rig wheel within the limitations provided by our sensors and motor strength. The assortment of wheel weights used throughout the test rig experiments demonstrates the ability for this technology to be useful on a variety of differently-sized rovers, both on the Moon and on Mars. As seen in table 1, the range of single-wheel weights used in our Earth-gravity testing correspond to a wide span of lunar and Martian rover masses. Notably, the weights tested account for 230-580 kg lunar rovers, which significantly match the class of rovers that CLPS providers are capable of landing. The range of Mars rover masses emulated also include the MER-family of rovers at 180 kg.

Weight on Test Rig Wheel (N)	Equivalent Lunar 4-Wheel Rover Mass (kg)	Equivalent Lunar 6-Wheel Rover Mass (kg)	Equivalent Martian 4-Wheel Rover Mass (kg)	Equivalent Martian 6-Wheel Rover Mass (kg)
91	225	337	98	146
122	302	452	131	196
158	389	584	169	254

Table 1 Representative rover masses for the different weights-on-wheel evaluated during single-wheel experiments.

Early tests were performed on loose hilly terrain without dictating a slip ratio, so the test rig wheel was commanded to move across the terrain at whatever slip it could manage. These tests demonstrated somewhat better performance by the deployed inflatable wheel compared to the rigid control wheel, especially when navigating the loose uphill slopes. Overall, the deployed inflatable appeared to traverse the hill and trough more easily and with less sinkage than the rigid counterpart. **A video highlighting the inflation and test runs of one of our early prototype wheels can be found here:** `https://youtu.be/C8fEwdTn2qs`

Once the test rig was fully outfitted with sensors and the capability to force a slip value, we collected performance data across a range of slip values that a rover may experience. This test compared the tractive (forward) force measured during a traverse over flat loose terrain across four different 28cm diameter wheel types: 1) a nominal rigid wheel, 2) a double-width rigid wheel equivalent to the width of our deployed inflatables, 3) a deployable inflatable without grousers, and 4) our final design of a deployable inflatable with grouser petals. The data collected follows expected curves from theoretical terramechanics - paradoxically, as slip increases, so does the forward tractive force until the wheel free-spins and digs itself into a hole. The data for tractive force is shown in figures 16-18.

The data reflects the fact that double-width wheels are not significantly better than their nominal width counterparts, which makes sense as they contribute high bulldozing resistances. Thus, we can save on wear and tear on the inflatable by keeping it stowed, while also not losing performance over terrain with good trafficability. The same tests also collected wheel torque data, shown in figures 20 & 21. Comparing the torque required to drive the two deployed inflatable wheels, the inflatable without grouser petals required substantially more torque on average to drive. This data reflects the benefits in torque transfer that the addition of deploying grousers provides.

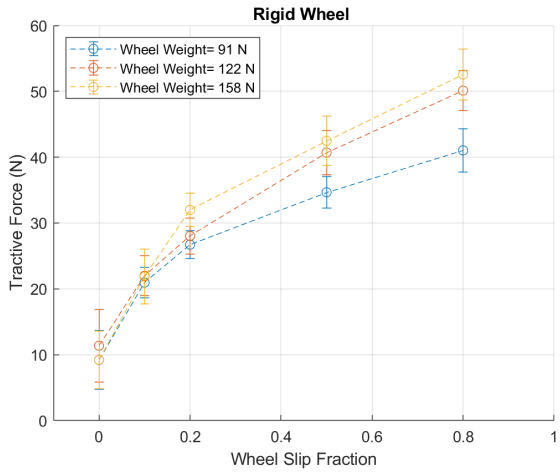

Fig. 16 28cm diameter, 10cm wide rigid wheel test

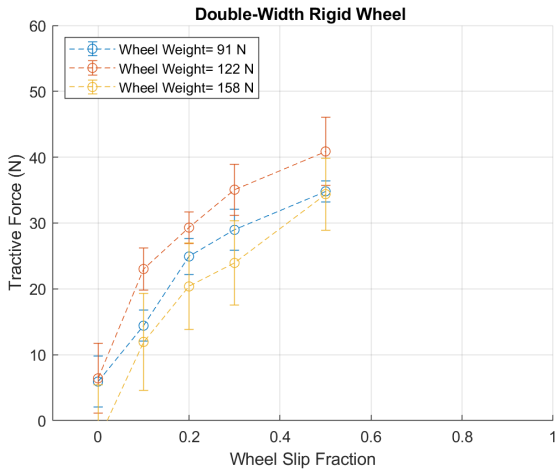

Fig. 17 28cm diameter, 20cm wide rigid wheel test

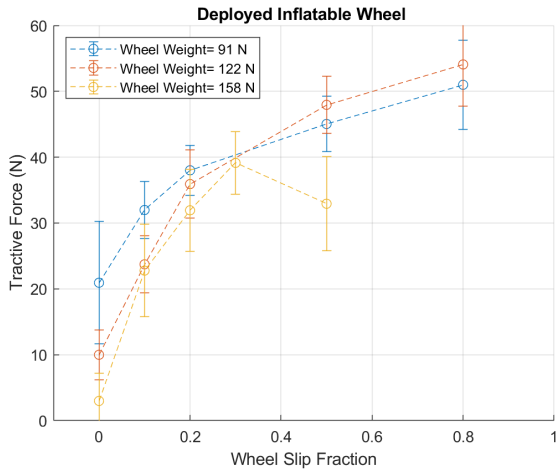

Fig. 18 28cm diameter wheel with 10cm-wide rigid section and 10cm deployed inflatable

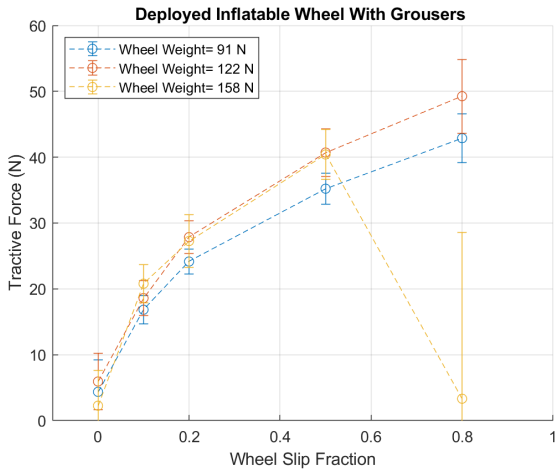

Fig. 19 28cm diameter wheel with 10cm-wide rigid section and 10cm deployed inflatable also with grouser petals

D. Integrated Rover Testing

In order to better understand the implications of AIRWHEEL in a complete rover system, the team wanted to fully outfit a rover with inflatable hubs and test it in typical rover operations. To stay within the budget and time constraints of BIG Ideas, we needed to adapt an existing rover rather than create a bespoke system. As a developmental test unit for the (long lost and lamented) RoboOps competition, the SSL has a 30 kg rover with a rocker suspension system and neutral-axis steering on all four wheels. The challenge was that it was designed for wheels almost exactly half the diameter of AIRWHEEL prototypes, which required the design, fabrication, and assembly of new steering arches for each of the wheels large enough to accommodate the bigger wheels.24 This was readily accomplished, and the vehicle was taken to a lunar analogue site (a volleyball sand court) for testing in loose soil. The soil at the testing location was shoveled and made into a slope and crater for the purposes of the testing. 22

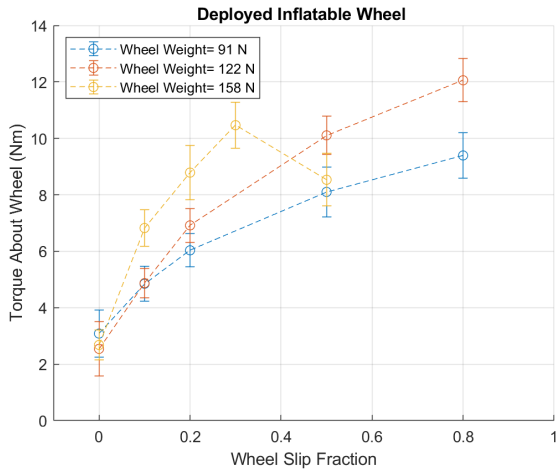

Fig. 20 28cm diameter wheel with 10cm wide rigid section and 10cm deployed inflatable without grouser petals

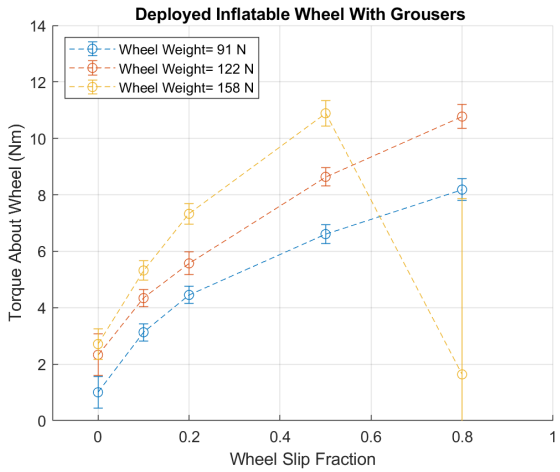

Fig. 21 28cm diameter wheel with 10cm-wide rigid section and 10cm deployed inflatable also with grouser petals

Our ASTRA (Adaptive System for Testing Rover Advancements) rover was tested on a 45 degree slope 23 made of loose soil. The test was done in two phases. The main procedure of this test was to drive ASTRA up the created slope until it was unable to move forward, and then inflate desired wheels before continuing up the slope and clearing the obstacle. The first phase involved only testing our remote inflation wheel, and thus comparing it to the non inflated rigid wheels that were left uninflated for the run while moving up the slope. The second phase was to follow the exact same procedure but inflate all wheels on the rover. The first phase shows, in video, that the inflated wheel has less slip on the slope than the rigid wheel on its opposing side. The same is true with the second test where one wheel was left uninflated for a similar reason. The third, additional run, on the field test was running through the track (after resetting each time) with all wheels inflated to begin with. ASTRA was found to cross over the ditch and slope with ease when all wheels were deployed during this test. (See Fig. 25)

E. Vacuum Testing

Due to the use of inflated components, the AIRWHEELS team felt it necessary to verify the functionality of the system in vacuum. History with systems such as ECHO or inflatable structures deployed from the Space Shuttle showed that even small volumes of air trapped inside the sealed chambers during pre-flight packing could create irresistible inflation pressures once in the vacuum environment, and we wanted to verify that AIRWHEELS would not have that issue. We also wanted to verify the functionality of the deflation system, which is basically a valve to open the pressure bladder to ambient and allow the internal gas to bleed into vacuum.

The auto-inflation system (described elsewhere in this report) uses a commercial CO_2 cartridge for the inflation process, controlled by one solenoid valve to allow the pressurized gas into the inflation bladder and a second solenoid valve to vent to ambient pressure. Since the test wheel was also used on both the wheel test rig and the integrated rover tests, as well as the fact that the structure was 3D printed from PLA, it had to be tested in a “dirty” chamber that allows test hardware that outgasses in exchange for lesser values of vacuum. Since the AIRWHEELS test was an operations

Fig. 22 Testing rover over slope with site seen

Fig. 23 Measured angle of the test slope using digital inclinometer

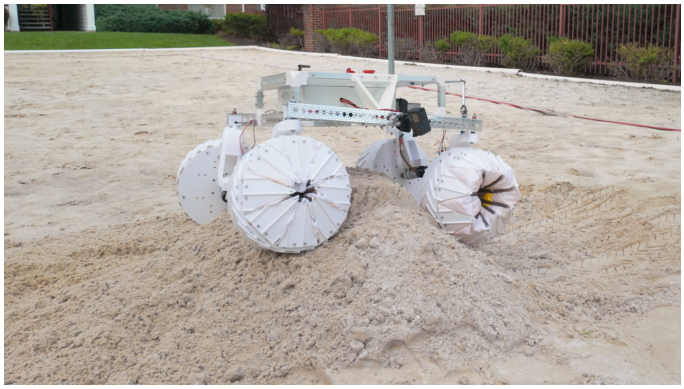

Fig. 24 ASTRA rover operating on slope with inflated wheel

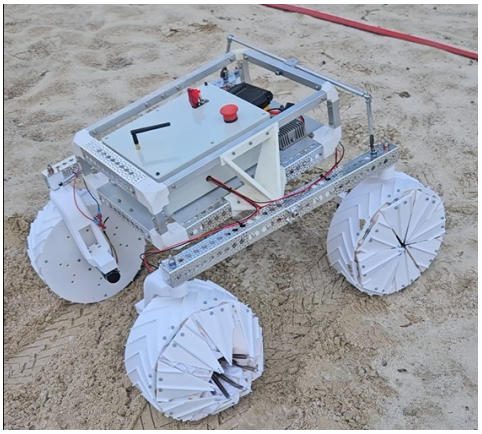

Fig. 25 Rover close-up

demonstration only, the fact that the ambient pressure was not down in the nano-torr range present on the Moon was not significant.

The Space Systems Laboratory recently received a thermal vacuum chamber as a donation from a local company which no longer needed it; this was designated to become the SSL "dirty" chamber and AIRWHEELS became its inaugural test case. At this point in time, neither the cryo pumps nor the cooling shroud are operational, but as stated previously, this was not important to the test objectives. The original desire was to put a miniaturized version of the wheel test rig in the chamber and verify wheel-soil interactions quantitatively under vacuum conditions, but the interior dimensions of the internal shroud structure (0.7 m diameter by 1.2 m long) did not accommodate a motion-based test rig, so the team settled for a static deployment and retraction.

The test was designed to collect photos and videos of the deployment and retraction process via a GoPro camera mounted in the vacuum chamber with the test wheel and shooting photos and videos handheld through a glass window in the chamber door. Due to lack of time, the exterior photography

has to contend for porthole space with a flashlight handheld by a second person illuminating the wheel for the photographer and the interior GoPro. Chamber pressure at the time of the test was manually recorded from a capacitive pressure transducer in the chamber.

V. Path-To-Flight

A. Materials Selection

Rover wheels for planetary surface applications have to withstand vacuum, temperature extremes, and environmental hazards such as regolith and rocks. Some aspects of flight materials are not feasible for this scale of experimental development, such as radiation-hardened electronics. However, some elements, such as the soft goods used here, have been designed and fabricated as close to flight specifications as practical given time, funding, and equipment limitations.

The rigid structures of the wheels were fabricated using fused deposition in enhanced PLA material. Due to the need for rapid revision and retesting of concepts, it was not practical to use metal of flight-certified additive manufacturing materials (e.g., Ultem, Windform XT) for this testing. Due to the critical nature of the soft goods, flight materials were used for this as feasible. The pressure bladders were fabricated from urethane-impregnated nylon material, similar to the pressure bladder in flight spacesuits. The accommodation made for the university laboratory was using heal seals for airtight assemblies, rather than radio frequency heaters used in spacesuit fabrication. The ideal material for the outer restraint layer would be the Ortho fabric used for the restraint layer and thermal/micrometeoroid garment of spacesuits; unfortunately, NASA is the sole customer for Ortho fabric and it cannot be procured commercially. For this reason, we used ballistic nylon fabric, which is a close match for Ortho fabric except for lacking the woven-in Kevlar reinforcing fibers. The materials selected were sufficient to allow testing in a thermal vacuum chamber, as described in more detail below.

B. Vacuum Testing

One of the primary objectives for AIRWHEEL testing was to test the deployment and restow procedures in vacuum. Required pressure levels are substantively changed by the ambient pressure; we wanted to ensure that we could package the wheel such that residual pressure in the inflation bladder did not prematurely deploy the auxiliary wheel when it reached vacuum, and that the venting of the bladder would be adequate to allow the passive springs to retract and stow the bladder after use.

Outgassing from the PLA material used to fabricate the wheel prevented the use of the "clean" thermal vacuum chamber in the SSL; however, the lab has recently received a surplus thermal vacuum chamber from a local company which is being installed and purposed as a "dirty" thermal vacuum chamber for use in testing wheel/soil interactions, robotic actuators, and any other components which would not be suitable for the "clean" chamber, or which do not require the 10^{-6} torr vacuum level achievable in that chamber. The new thermal vacuum chamber is still in the process of being installed in the SSL Advanced Robotics Development Laboratory, and the thermal aspect of it is still not functional, which was not an issue for the desired vacuum test.

The test wheel was installed in the chamber with a GoPro camera and the system was pumped down to 4.3 torr. The inflation process are triggered by a radio-control remote, causing the CO_2 cartridge pressure to fill the inflation bladder and deploy the auxiliary wheel. This test was highly successful, with the grouser pads and inflatable wheel deploying in about 10 seconds. Deflation and stowage was hampered by the lack of a visual indicator of the solenoid valve status, making it unclear whether the retraction was successfully commanded or not. The wheel system did begin the retraction, but it has been noted that retraction can take several minutes even in the laboratory

environment. Further research and development will take place to augment the bladder vent system to make the retraction both faster and more robust.

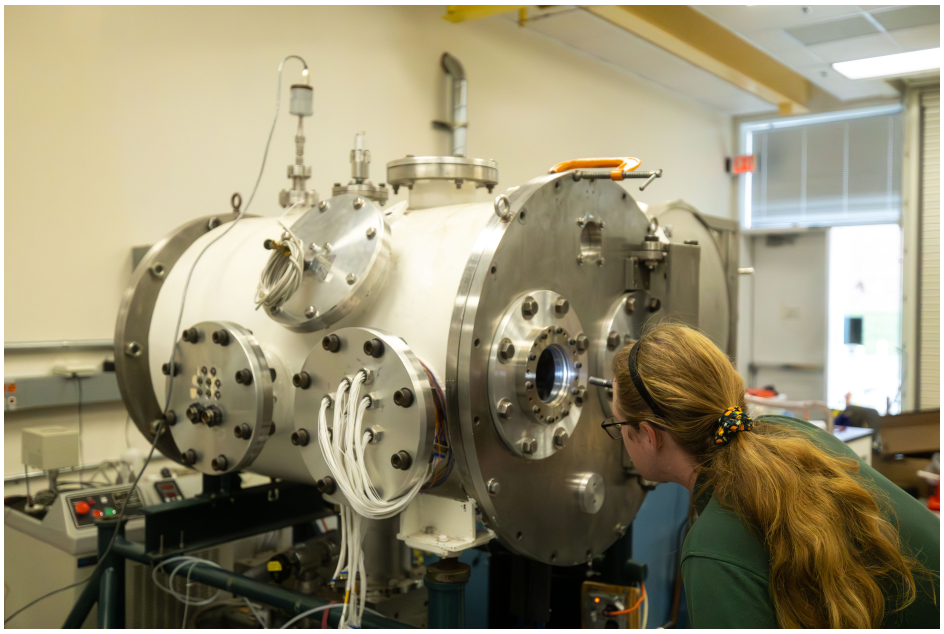

Fig. 26 The Space Systems Lab's thermal vacuum chamber while running a wheel deployment test

C. Wireless Power Transfer

When designing the power system, particular attention was paid to ensuring that the design would be feasible for flight conditions. One of the prevailing concerns was the temperature swings experienced at the lunar surface, which due to the exposed nature of the wheel present an extremely harsh endowment to any electronics contained within. For this reason, the choice was made to make the wireless power transfer system use only basic components on the receive side. The transmit side was permitted to use integrated circuits, due to being enclosed in a more controlled environment. To demonstrate the ability of a simple circuit to pick up and utilize the power from the transmit coil, a testbed (Figure 13) was constructed. The setup is a COTS wireless power transmitter, with the transmit and receive coils separated by a 2mm gap. The receive side of the circuit is a full bridge rectifier, with a pair of capacitors. The receive coil inductance and matched capacitor form a tank circuit that oscillates at 220kHz, which is the drive frequency of the transmit coil. The power from the receive LC tank is then rectified by the full bridge rectifier, and smoothed out by another capacitor. The rectified and smoothed power is used to power a 2W gas solenoid, which is the exact same model used in the wirelessly controlled inflatable wheel prototype. While this demonstrator is only 40% efficient, outputting 2W with an input of 5W, it demonstrates the ability to pass power though a non-contact system. Part of the efficiency loss was identified to be in the diodes, as due to a very large recovery time, they were not able to fully block current when reverse biased.

VI. Project Management

A. Organizational Structure and Processes

The AIRWHEEL project was organized and executed within the University of Maryland Space Systems Laboratory, taking advantages primarily of the facilities and infrastructure of that lab. The project was directed and performed by the student team members, with the laboratory director acting as principal investigator (responsible to the university for the project) and mentor. The organizational structure and major assignments were:

Dr. David Akin	Principal Investigator, Faculty Mentor
Nicolas Bolatto	Team Lead, Chief Engineer
Meredith Embrey	Soft Goods Lead
Daniil Gribok	Electronics Lead
Ryan Mahon	Wheel & Mechanisms Lead
Romeo Perlstein	Software Lead

All other project participants are included on the team list at the front of this report. Minor communications and files were handled through a Microsoft Teams channel that all members had access to. Major discussions and group decision-making was managed at either the laboratory's weekly general meetings, or at the additional BIG Idea project-specific weekly meeting.

B. Project Timeline

Final Timeline

PHASE	Subcategory	Task	Start	End	Weeks
Spring	Inflatable Wheel Initial Design and Development	Initial Wheel Fabric Patterns and Design Completion	1-Mar	15-Mar	3
		Inflatable Wheel Sealing Method Initial Testing and Interation	11-Mar	25-Mar	3
		Initial Pressure Bladder and Restraint Layer Fabric Sourcing	4-Mar	11-Mar	2
		Initial Wheel Fabrics and Parts Quote Retrival and Order Planning	18-Mar	22-Mar	1
		Initial Wheel Fabrics and Parts Order	25-Mar	29-Mar	1
	Outer Rigid Wheel Initial Design and Development	Rigid Wheel Design Parameter finalization (Radius, Width, Mounting, Etc.)	18-Mar	1-Apr	3
		Rigid Wheel Initial Deployable Grouser Design Iteration	8-Apr	15-Apr	2
		Rigid Wheel Grouser Parameter Design Iteration	8-Apr	22-Apr	2
		Inflatable Wheel Housing Design Finalization	1-Apr	15-Apr	3
	Wheel Test Rig Upgrade Finalization	Wheel Test Rig Software Development	29-May	6-Oct	23
		Wheel Test Rig Component Upgrades Finalization	11-Mar	25-Mar	3
		Wheel Test Rig Part Quote Retrieval and Order Planning	25-Mar	8-Apr	3
		Wheel Test Rig Part Order	8-Apr	-	1
	First Installment of Stipends		**Mar-24**		
	Outer Rigid Wheel Initial Design Finalization	Rigid Wheel Grouser Parameter Finalization (Grouser Height, Shape, Etc.)	29-Apr	-	1
		Rigid Wheel Deployable Grouser Design Finalization	22-Apr	-	1
		Rigid Wheel Initial Part Quote Retrieval and Order Planning	6-May	13-May	2
		Rigid Wheel Initial Part Order	13-May	-	1
	Inflatable Wheel Initial Design Finalization	Seal Testing and Inflation Method Verification	1-Apr	8-Apr	2
		Initial Inflatable Wheel Fabrication: Pressure Bladder and Restraint Layer	15-Apr	22-Apr	2
		Arrival: Initial Wheel Fabrics and Parts	8-Apr	-	1
	Outer Rigid Wheel Further Design and Development	Rigid Wheel Initial Fabrication	1-Apr	-	1
		Initial Grouser Deployment Testing and Iteration	22-Apr	29-Apr	2
		Rigid Wheel Deployable Grouser Final Design Development	6-May	13-May	2
		Rigid Wheel Grouser Retraction System Conceptial Development	15-Apr	29-Apr	2
	Inflation and Pressure Control System (IPCS) Initial Design and Development	Design Considerations and Conceptial Trade Studies	18-Mar	1-Apr	3
		System Parameter Estimation and Modeling	15-Apr	6-May	4
		Testbed Inflation Mechanism Design Finalization	1-Apr	8-Apr	2
		Testbed Inflation Mechanism Part Quote and Order Planning	8-Apr	-	1
		TestBed Inflation Mechanism Part Order	15-Apr	-	1
Summer	Wheel Test Rig Upgrades and Testing	Electical and Software Checkouts and Initial Data Validation	22-Apr	-	1
		Installation of Upgraded Parts	22-Apr	29-Apr	2
		Rigid Wheel Initial Design Testing	29-Apr	6-May	2
	Full-Time Students Arrival	Full-Time Summer Student Work Begins	27-May	19-Aug	-
	Second Installment of Stipends		**Jun-24**		
	Inflatable Wheel Design Finalization	Final Wheel Pattern Design Finalization	13-May	20-May	2
		Sealing Method Finalization	13-May	27-May	3
		Wheel Fabrics and Parts Quote Retrival and Order Planning	27-May	3-Jun	2
		Wheel Fabrics and Parts Order	10-Jun	-	1
	Inflatable Wheel Retraction System Design Finalization	Retraction System Parts Quote Retrival and Order Planning	20-May	27-May	2
		Retraction Systems Parts Order	27-May	-	1
	Wheel Test Rig Software And Data Validation	Continued Data File Output Validation	26-Aug	-	1
		Sensor Calibration and Validation	26-Aug	2-Sep	2
		System Intelligence Upgrades and Further QOL additions	26-Aug	30-Sep	6
	Inflatable Wheel Fabrication and Validation	**Arrival**: Wheel Fabrics and Parts	1-Jul	-	1
		Single Inflatable Wheel Fabrication	8-Jul	15-Jul	2
		Inflatable Wheel Inflation Test and Seal Validation	22-Jul	5-Aug	3
		Inflatable Wheel Integration with Rigid Wheel	12-Aug	-	1
	Wheel Testing	Initial Rigid Wheel Testing (No Inflatable)	5-Aug	19-Aug	3
		Initial Rigid Wheel Testing (Inflatable + Grousers)	19-Aug	2-Sep	3
Fall	Continued Wheel Testing On Linear Test Rig	Slip Charactertization of Rigid Wheel Only	26-Aug	2-Sep	2
		Inflatable Wheel Testing (No Deployed Grousers)	9-Sep	16-Sep	2
		Slip Characterization of Rigid Wheel + Deployed Inflatable (With Grousers)	16-Sep	23-Apr	2
		Drawbar Pull of Rigid Wheel	26-Aug	16-Sep	4
		Drawbar Pull of Rigid Wheel + Inflatable	9-Sep	26-Sep	3
		Inclined Performace Testing of Rigid Wheel vs Rigid + Deployed Wheel	30-Sep	14-Oct	3
		Recovery Testing of Inflatable Wheel with Stuck Rigid Wheel	30-Sep	7-Oct	2
	Inflatable Wheel Retraction System Testing and Integration	**Arrival**: Retraction Systems Parts	17-Jun	-	1
		Retraction System Integration (Single Wheel)	8-Jul	15-Jul	2
		Retraction System Testing, Validation, Modification	8-Jul	5-Aug	5
		Retraction System Integration (4 Wheels)	5-Aug	19-Aug	3
		Retraction System Stow-Unstow Analysis	12-Aug	26-Aug	3
	On-Wheel IPCS Integration and Initial Testing	IPCS Single Wheel Integration and Testing, Validation, Modification	5-Aug	19-Aug	3
		IPCS Final Integration (4-Wheels)	26-Aug	16-Sep	2
		Thermal Vacuum Testing of Inflation and Deflation	11-Oct	12-Oct	1
	4-Wheel Rover Inflatable Wheel Development	Inflatable Wheel Fabrication: Pressure Bladder and Restraint Layer	18-Sep	23-Sep	3
		Inflatable Wheel Inflation Testing and Seal Confirmation	23-Sep	30-Sep	2
		Inflatable Wheel Integration (4-Wheels)	23-Sep	21-Oct	2
	4-Wheel Rover Modifications and Outfitting	Steering Arch and Wheel Mounting Modifications	30-Sep	1-Oct	3
		Wheel Integration and Initial Checkouts	30-Sep	1-Oct	1
	4-Wheel Rover Testing	Rover Testing with Rigid Wheels (No Inflation)	13-Oct	14-Oct	1
		Rover Testing With Rigid Wheels + Deployed Inflatable (Grousers)	13-Oct	14-Oct	2
	Documentation	Mid-Project Report (MPR)	1-Apr	4-Jun	9
		IPCS Documentation			5
		Fabric Pattern, Sealing, and Sewing Documentation			14
		Wheel Characteristic Documentation			21
		Fall Status Report Deadline			7
		Technical Paper and Tech Verification Demo			6
		Presentation and Digital Poster			6

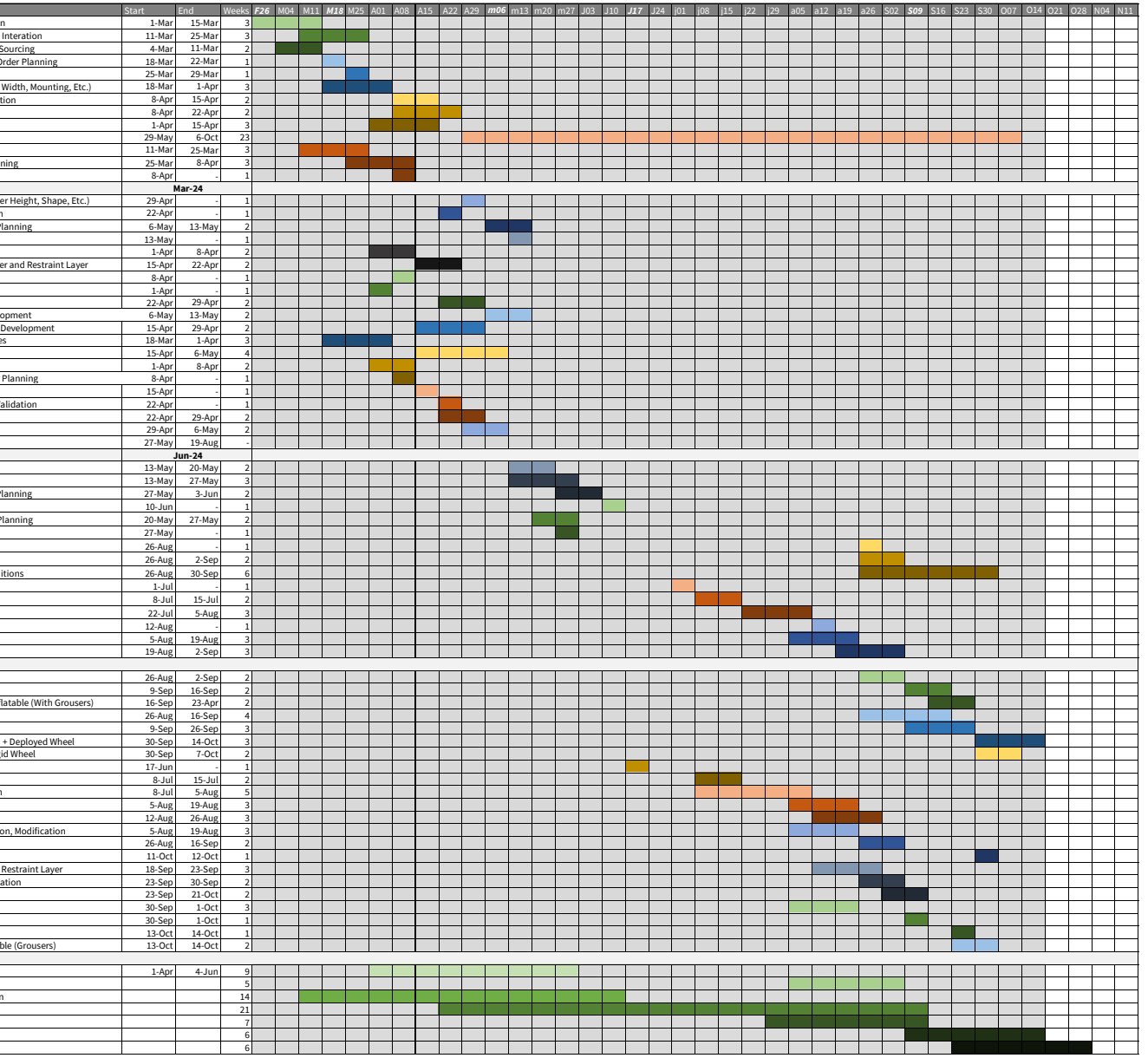

C. Detailed Budget

This section must be prefaced with the fact that as of this submission, *the University of Maryland still has NOT received the BIG Idea Phase 2 funding from Maryland Space Grant.* We understand that it is "held up in paperwork" at the home university of Maryland Space Grant. All expenditures and encumbrances listed here for Phase 2 have actually been internally funded by the University of Maryland with the expectation (hope?) of transferring the expenses to the BIG Idea Phase 2 funds when (if?) they arrive.

Category	Phase 1	Phase 2
Supplies/Materials	$6182	–
Salaries and Benefits	$16,187	$12,000
IDC	$12,526	–
Encumbrances	$11,574	$13,890
Projected Travel	–	$10,325
Projected Balance	$28,483	$38,785

Table 2 Detailed Budget

Current encumbrances cover personnel and known expenses to the original end of the contract period. We have arranged with Maryland Space Grant that *when* the Phase 2 funding arrives, the Phase 2 period of performance will be extended to April 22, 2025. We plan to use the projected balances to continue this project until that date. It should also be noted that the principal investigator purposefully slowed expenditures in the last three months against the (hopefully faint) possibility that the Phase 2 funds would *never* show up, reserving enough Phase 1 funds to meet our obligations to finish the project and compete at the final symposium in Las Vegas in November.

References

[1] Terzaghi, K., Peck, R. B., and Mesri, G., *Soil mechanics in engineering practice*, John wiley & sons, 1996/1948 First Edition. URL https://books.google.com/books?hl=en&lr=&id=XjH6DwAAQBAJ&oi=fnd&pg=PR19&dq=terzaghi&ots=ahNzO3Pc8G&sig=IFEkc9N0oEyjE2khzEWNEIcgEZA#v=onepage&q=terzaghi&f=true.

[2] Bekker, M., *Introduction to Terrain-vehicle Systems*, University of Michigan Press, 1969. URL https://books.google.com/books?id=J31TAAAAMAAJ.

[3] Wong, J. Y., *Theory of Ground Vehicles*, Wiley-Interscience, 2001 (Original 1978). https://doi.org/10.1243/095440702760178640.

[4] Reece, A. R., "Principles of Soil-Vehicle Mechanics," *Proceedings of the Institution of Mechanical Engineers: Automobile Division*, Vol. 180, No. 1, 1965, pp. 45–66. https://doi.org/10.1243/PIME_AUTO_1965_180_009_02, URL https://doi.org/10.1243/PIME_AUTO_1965_180_009_02.

[5] Maimone, M., Cheng, Y., and Matthies, L., "Two years of Visual Odometry on the Mars Exploration Rovers," *Journal of Field Robotics*, Vol. 24, No. 3, 2007, pp. 169–186. https://doi.org/10.1002/rob.20184, URL https://onlinelibrary.wiley.com/doi/10.1002/rob.20184.

[6] Toupet, O., Biesiadecki, J., Rankin, A., Steffy, A., Meirion-Griffith, G., Levine, D., Schadegg, M., and Maimone, M., "Terrain-adaptive wheel speed control on the Curiosity Mars rover: Algorithm and flight results," *Journal of Field Robotics*, Vol. 37, No. 5, 2020, pp. 699–728. https://doi.org/10.1002/rob.21903, URL https://onlinelibrary.wiley.com/doi/10.1002/rob.21903.

[7] Goodman, R., and Peck, R., *Karl Terzaghi: The Engineer as Artist*, ASCE Press Series, American Society of Civil Engineers, 1999. URL https://books.google.com/books?id=QgdJIAVT1_UC.

[8] Iagnemma, K. D., Rzepniewski, A., Dubowsky, S., Pirjanian, P., Huntsberger, T. L., and Schenker, P. S., "Mobile robot kinematic reconfigurability for rough terrain," *SPIE Proceedings*, edited by G. T. McKee and P. S. Schenker, SPIE, 2000. https://doi.org/10.1117/12.403739.

[9] Apostolopoulos, D., Wagner, M. D., Heys, S., and Teza, J., "Results of the inflatable robotic rover testbed," *Robotics Institute Carnegie Mellon University*, Vol. 5000, 2003.

[10] Girija, A. P., Agrawal, R., Lu, Y., Arora, A., de Jong, M., Saikia, S. J., and Longuski, J. M., "A single wheel test rig for ocean world rovers," *Journal of Terramechanics*, Vol. 109, 2023, pp. 101–119.

[11] Apostolopoulos, D., "Analytical Configuration of Wheeled Robotic Locomotion," 2001.